Borehole thermal response and thermal resistance of four different grouting materials measured with a TRT

Borinaga-Treviño, R, Pascual-Muñoz, P, Castro-Fresno, D & Blanco-Fernandez, E

Original citation & hyperlink:
Borinaga-Treviño, R, Pascual-Muñoz, P, Castro-Fresno, D & Blanco-Fernandez, E 2013, 'Borehole thermal response and thermal resistance of four different grouting materials measured with a TRT' Applied Thermal Engineering, vol. 53, no. 1, pp. 13-20.
https://dx.doi.org/10.1016/j.applthermaleng.2012.12.036

DOI 10.1016/j.applthermaleng.2012.12.036
ISSN 1359-4311
ESSN 1873-5606

Publisher: Elsevier

Author's post-print: Borinaga-Treviño, R., Pascual-Muñoz, P., Castro-Fresno, D., Blanco-Fernandez, E. "Borehole thermal response and thermal resistance of four different grouting materials measured with a TRT". Applied Thermal Engineering 53 (1), pp. 13-20. ISSN: 1359-4311.

Borehole thermal response and thermal resistance of four different grouting materials measured with a TRT

Borinaga-Treviño, Roque[a]; Pascual-Muñoz, Pablo[a]; Castro-Fresno, Daniel[a]; Elena Blanco-Fernande[z]

[a] *Department of Transports, Projects and Processes Technology, University of Cantabria, Spain.*

ABSTRACT

Among other systems, closed-loop geothermal heat exchangers are extensively used due to the lower environmental impact compared to open-loop systems. Thermal conductivity is the main parameter required for the design of the geothermal heat exchangers, which is determined by the Thermal Response Test (TRT). However, in most of the design cases only one TRT is done per project because of its cost. Therefore, there is no available data to contrast with the measured ones and the data obtained must be taken as valid. 4 different TRTs are executed in 4 different boreholes to analyze the reliability of the estimated thermal conductivity. Each of the boreholes tested has similar geological and geometric characteristics, but the grouting material is different in each of them. Basic Oxygen Furnace (G2), Silica sand (G3) and Construction and Demolition Waste (G4) have been used as base aggregates in cement based self-compacting mortars, and compared with a cement-bentonite-graphite (G1) grouting material. Results indicate that thermal conductivity of the ground is between 2.2 W/(m·K) and 2.58 W/(m·K). However, this value is influenced by the water content of the ground during the performance of the test. According to the Borehole Thermal Resistance (R_b), the G1 mix performs the best, but G4 has similar values. Laboratory measured grout thermal conductivity has not been a good estimation parameter for the determination of the R_b, since contact resistance between the pipes and the grout is of importance due to the shrinkage of the cement based mixes.

KEYWORDS: Grout; Borehole Thermal Resistance; Mortar; Thermal Response Test; BTR; TRT.

1. INTRODUCTION

According to Omer [1], 40% of the world's energy consumption takes place in heating, cooling and lighting of buildings. Therefore, efficiency improvements are necessary to prevent or at least reduce global warming. On the one hand, buildings must be well insulated to reduce energy loss and hence improve thermal efficiency. On the other hand, renewable energy sources must be implemented to reduce the use of fossil fuels. Ground-Coupled Heat Pumps have proved to be a reliable, efficient system for heating and cooling buildings [2] and for snow melting of pavement surfaces [3-5]. Heat stored in the ground is considered as a renewable energy when a GCHP system is used, and its greenhouse gas emissions are due to the way of producing the electricity required by the system. For instance, greenhouse gas emissions could be zero if the required electricity is provided by other renewable energies, such as solar or wind energies.

GCHP systems consist of a closed-circuit, pipe system buried in the ground that exchanges heat with it. To ensure borehole wall stability and a proper heat transmission to/from the ground, a grouting material is normally injected. Therefore, during the design of a vertical closed-loop Ground Heat Exchanger (GHE), thermal properties of the ground, grout and pipe system must be taken into consideration. Thermal properties of the ground are the most important parameters for the design of GHEs, and they are determined in situ by a Thermal Response Test. This test consists in injecting a constant heat flow measuring the increment in temperature with time in order to study the thermal response of the ground [6]. Most of the methods proposed to estimate the thermal behavior of the GHE from the TRT-data are summarized by Rainieri et al. [7]. Many of them use the thermal conductivity of the ground and borehole thermal resistance to define the GHE thermal properties.

Ground thermal properties depend on the location of the installation, so the efficiency of the GHE cannot be improved with a better ground disposal. Therefore, GHE efficiency should be improved by using high thermal conductivity grouting materials. On the one hand, Allan et al. [8-12] analyzed the applicability of cement-based mortars as grouting material, concluding that cement superplasticized silica sand mortars improved the GHE thermal efficiency with respect to the cement or bentonite alone mixes. On the other hand, due to its thixotropic behavior, bentonite-based grouts have been more widely analyzed. Chulo et al. [13] and Delaleux et al. [14] used graphite and silica sand to improve the thermal conductivity of the bentonite-based grouting materials to values higher than most of the ground's values but its real influence on the GHE efficiency has not yet been analyzed by the authors.

Other authors have analyzed the influence of the borehole properties on the logged temperature during a TRT. Marvin et al. [15] analyzed the influence of the ground thermal conductivity, grout thermal conductivity and borehole diameter on the thermal performance of the GHE. Marvin concluded that a higher thermal conductivity of the grout reduced the thermal resistance of the GHE and hence enhanced its performance. Accordingly, Zang et al. built 3 Vertical Heat Exchangers to determine the influence of the grouting material in the resulting circulating water temperature [16]. Borehole depth, diameter and piping were similar in all of them, but the grouting materials were bentonite, enhanced bentonite/ sand mixture and natural limestone drill cuttings. By using an initial time of 1 h, the estimated effective thermal conductivity of the ground increased as the effective thermal conductivity of the grout increased, indicating that the two parameters were correlated. Lee et al. [17] compared different borehole arrangements, varying both grouting material and pipe layout. For the grouting materials, they varied the main material (cement or bentonite) and the additives (silica sand and/or graphite), and they also compared two different pipe dispositions (Simple U and a new 3 pipe type). By performing 6 TRTs, they determined that improvements in the grouting materials and pipe disposition enhanced the effective thermal conductivity of the ground.

This paper has two main objectives: i) to determine the variability of the predicted ground thermal conductivity for the same evaluated ground and ii) to determine the influence of the type of grout used in the estimated borehole thermal resistance.

2. EXPERIMENTAL PROCEDURE

Four TRTs have been performed in 4 different borehole heat exchangers, each of them containing a different grouting material, to determine the thermal conductivity of the ground and the borehole thermal resistance.

2.1. Grouting materials

Table 1 shows the mix proportions used in this contribution. Mix proportions are calculated based on the results obtained in a previous work [18]. Due to material unavailability, Limestone based mix was replaced by a 40% solid cement-bentonite-graphite commercial mix (G1), which is chosen as reference material. Exact proportions of its components are unknown, although the manufacturer lists a thermal conductivity of 1 W/(m·K). For the same reason, Electric Arc Furnace slag aggregate was also replaced by Basic Oxygen

Furnace sand (BOF, G2 mix). BOF proportion in the G2 mix is recalculated to ensure the required consistency without experiencing segregation problems. Finally, Silica sand (S, G3 mix) and Construction and Demolition Waste (CDW, G4 mix) based mix proportions are the ones proposed in Ref. [18]. For cement-based mix proportions (G2, G3 and G4), 2% of melamine-based superplasticizer (SP) was used to reduce water content and segregation of the mixes. However, during the laboratory testing an unusual early set was observed in the G2 mix, so 1% of set retardant (SR) was added to the mixes. Finally, to correct the high water-sensitivity of the mix caused by the SP, 4% bentonite (B) by unit weight of cement was also added to the mix.

Table 1. Mix proportions and laboratory measured grout thermal conductivity for the boreholes tested.

	Grouting material			
	G_1	G_2	G_3	G_4
Cement (c)	CEM III/B 32.5R/SR (UNE-EN 197-1)			
Aggregate 1 (A1)	Graphite	BOF	S	CDW
A1/c	Unknown	1.25	3.0	1.80
Aggregate 2 (A2)	-	LF	-	LF
A2/c	0	0.75	0	0.20
Bentonite	High Montmorillonite content			
B/c	Unknown	0.04	0.04	0.04
Water to cement ratio (w/c)	0.4*	0.55	0.52	0.50
Superplasticizer (SP)	None	Melment F10®		
SP/c	0	0.02	0.02	0.02
Set Retardant (SR)	None	Rheomix 925®		
SR/c	0	0.01	0.01	0.01
Oven dried Thermal conductivity (W/(m K))	0.6	0.8	1.1	0.8
Water saturated thermal conductivity (W/(m K))	1.1	0.9	1.6	1.2

*Water to total solids ratio by weight

Prior to the execution of the TRTs, apparent thermal conductivity of the injected mixes was determined in laboratory, according to the ASTM D-5334 standard [19]. 3 specimens per grouting material were created and cured at ambient temperature for 2 days until the removal of the molds was possible. From then until the end of the curing period (14 days), specimens were cured by submerging them in water at 20 °C. Once the curing age was reached, specimens were first tested submerged in water to ensure water saturation conditions. To determine the dry thermal conductivity of the grouts, specimens were oven dried for 48 h at 105 °C and exposed at ambient room temperature (20 °C) for 1 week to reach thermal equilibrium before carrying out the tests. The results obtained are listed on Table 1. As G1 is a bentonite-based mix, it undergoes greater loss of thermal properties when oven dried than any of the cement-based grouting materials. During the drilling of the boreholes, it was observed that groundwater level was close to the foundation's lower limit; hence a saturated ground is assumed. Therefore, water-saturated grout thermal conductivity values are taken into account.

2.2. Ground heat exchangers

Tested boreholes are part of a ground heat exchanger system designed for a future office building. All the boreholes are approximately 98 m deep and have a borehole diameter (d_b) of 120 mm. 32/26.2 mm outside/inside diameter ($d_{p,o}/d_{p,i}$) PE100/SDR11 double U pipe system is inserted with an imposed shank spacing (s) of 57 mm, because of the presence of the 25mm diameter grout injection pipe. No spacers have been used to place the piping unit in the center of the borehole, so its position inside the borehole is initially unknown, but it is assumed to be centered on average with respect to the borehole walls. The final situation of the tested boreholes is highlighted in Fig. 1.

Once construction of the boreholes was finished, a minimum of 14 days was allowed to pass to avoid altering the curing of the grouting materials, which could affect the results of the test due to the hydration of the cement paste. To avoid thermal interference among the consequent tests, a minimum of 7 days was allowed before carrying out the next test. The order of the tests was also chosen to minimize the thermal effect of one test on another.

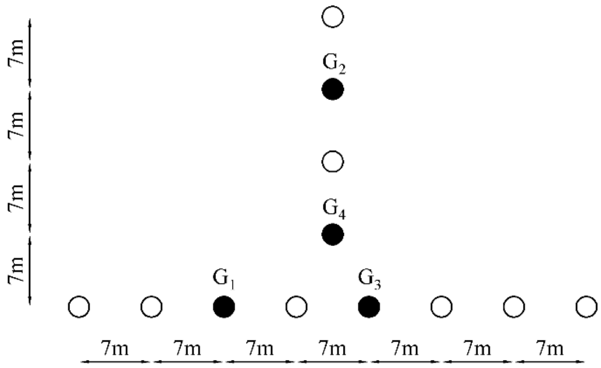

Fig. 1. Position of the Thermal Response Tests in the resulting bore field.

2.3. Thermal Response Test

Before carrying out the test, vertical temperature along the borehole is measured to determine the initial undisturbed ground temperature profile. For that purpose, an “In situ Level troll 500 series” device was chosen, which measures temperature and depth in existing aquifers with an error of 0.1 °C and 0.1 m. Fig. 2 shows the device and a detailed sketch of the measuring procedure.

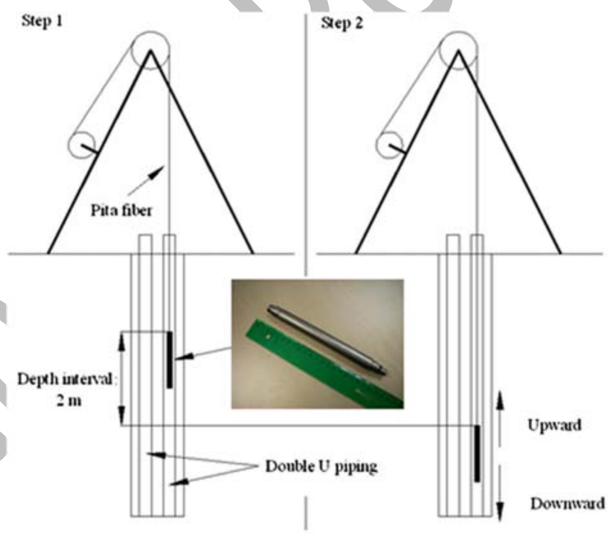

Fig. 2. Temperature measurement profile device.

Device is descended along one of the four pipes, and stopped approximately every 2 m depth interval for at least 15 s. Since the device loges the data every 5 s, temperature for each 2 m depth interval is determined as the mean of at least 3 measured values. As a result, four different vertical temperature profiles are determined, one for each TRT, in order to be able to discard thermal interference among the TRTs. The results also provide the depth from which ambient temperature does not affect the ground temperature, and indicate that the thermal gradient underground is linear. Once both thermal conductivity of the ground and temperature gradient with depth (DT/DH) are known, the earth’s internal heat flux (EHF) is calculated by using equation (1). The results are then compared to the value estimated for the area by the European atlas of geothermal resources [20].

$$EHF = \lambda_{ground} \cdot \Delta T / \Delta H \tag{1}$$

Fig. 3 shows the TRT equipment used and its main components. When carrying out a Thermal Response Test, a constant heat is injected in the ground by imposing a constant heating capacity and water circulation. A heating deposit with 3 independent 3 kW electric heaters is installed at the bottom part of the equipment. A constant flow water circulating pump is installed, and the required flow can be regulated by a manually operated valve. A Kobold DRG 1860 flow meter with an accuracy of ±3% is used to measure the flow, whose data is registered by a Testo 175-S2 data logger. K-type thermocouples (with an accuracy of ±0.3 °C) determine the inlet and outlet water temperatures and the data is logged in the Testo 177-T4 data logger.

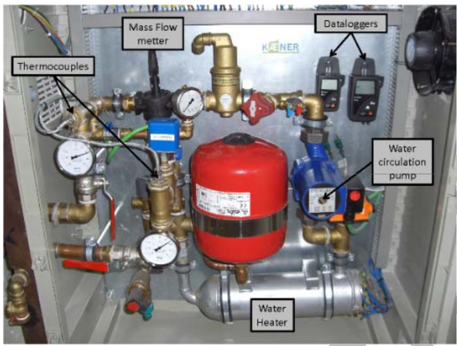

Fig. 3. Description of the TRT equipment used.

During the tests, a constant heating power (Q) of 6 kW is imposed in the heater. The turbulent regime and constant heat injection is ensured by choosing a constant water flow rate of 16 l/min. Duration of the test depends on the chosen estimation method. Rainieri et al. present a critical review of all the existing analytical and numerical methods to evaluate the ground and borehole thermal properties from the in situ measured data. Among all the available methods, apparent ground thermal conductivity and borehole thermal resistance are determined by the Infinite line source theory (ILS), due to its simplicity and extensive use. The main disadvantage of the ILS over more detailed methods is that it is not able to model the geometry of the borehole. As all the boreholes studied have the same length and geometry, borehole thermal resistance values can be compared directly and therefore ILS method is considered as valid. This theory assumes that the vertical heat exchanger is an infinite line inside a homogeneous semi-infinite medium, with no heat storage capacity. If constant heat flux and radial heat flow are supposed, the approximate analytical solution is given by Mogensen et al. [21], which is shown in equation (2). Tm, T1 and T2 are the mean, inlet and outlet temperatures of the heat carrier fluid. T0 is the initial temperature of the ground determined as the mean temperature of the vertical temperature profile measured previously. γ is Euler's constant (0.5772), m and C_p are the mass flow rate and specific heat capacity of the circulating fluid, and d_b is the mean borehole diameter. H, λ_{ground} and R_b are the depth of the borehole, apparent thermal conductivity of the ground and borehole thermal resistance, respectively. Finally, α is the thermal diffusivity of the ground (m2/s). The slope of the temperature profile against the Napierian logarithm of time (k) permits the calculation of the apparent thermal conductivity of the ground (3). The ILS provides a valid result for apparent thermal conductivity with a maximum error of 2% if the initial time satisfies the condition showed in equation (4).

$$T_m = T_0 - \frac{mc_p(T_1 - T_2)}{4\pi\lambda_{ground}H}\left[\ln\left(\frac{\alpha t}{d_b^2}\right) - \gamma\right] + \frac{mc_p(T_1 - T_2)R_b}{H} \tag{2}$$

$$\lambda_{ground} = -\frac{Q}{4\pi H k} \tag{3}$$

The thermal conductivity of the ground is calculated based on the minimum and maximum times recommended by Gehlin et al. equations (4) and (5) [22]. As thermal diffusivity is unknown, an estimation of its value is necessary to determine the initial and final times for the regression analysis. Thermal diffusivity can be estimated by knowing the thermal conductivity and the volumetric heat capacity of the ground. Taking into account that the ground consists of water-saturated clay with sand grains, the specific volumetric heat capacity of the ground is estimated based on the VDI 4640 standard [23]. The mean value observed for saturated sands is $2.4 \cdot 10^6$ J/(m3·K). The thermal conductivity of the ground is initially unknown and an iterative process should be done, but in this case, a ground thermal conductivity (λ_{ground}) of 2.5 W/(m·K) was expected from previous experience in the area. Based on all these assumptions, a thermal diffusivity (α) of $1.1 \cdot 10^{-6}$ m2/s was determined. Based on equations (4) and (5), and a borehole diameter of 12 cm, an initial minimum time of 5 h and a minimum test duration of 48 h are calculated.

$$t_{min} \geq \frac{5d_b^2}{4\alpha} \tag{4}$$

$$t_{max} \geq \frac{50d_b^2}{4\alpha} \tag{5}$$

As considered by the ILS method, fluid mean temperature evolution is used to determine the borehole thermal resistance, which is estimated using equation (6). Final R_b value is calculated as the mean of the 5-48 h time gap instantaneous R_b values. Assuming that all the pipes have the same temperature, borehole thermal resistance is equivalent to the four pipe thermal resistances acting in parallel [24]. Fig. 4 shows the resistance model used, as well as the associated equation (7).

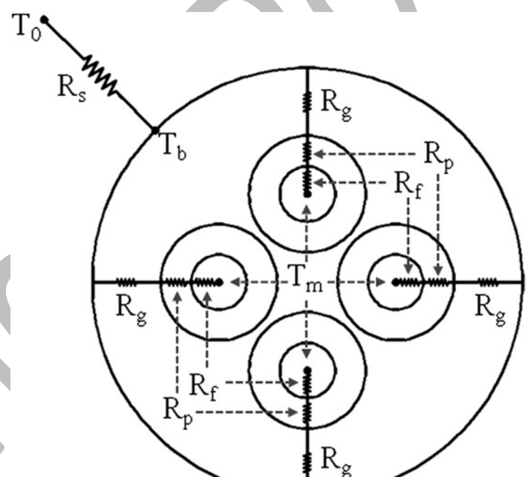

Fig. 4. Thermal resistance model used for the estimation of R_b.

$$R_b = \frac{H}{Q}\left(T_m(t) - T_0\right) - \frac{1}{4\pi\lambda_{ground}}\left(\ln\left(\frac{\alpha t}{d_b^2}\right) - \gamma\right) \tag{6}$$

$$R_b = (R_f + R_p + a_{p-g} + R_g)/4 \tag{7}$$

Where: R_f is the fluid to pipe convection resistance in (m·K)/W; R_p is the pipe thermal resistance in (m·K)/W; a_{p-g} is the pipe to grout contact resistance in (m·K)/W; R_g is the thermal resistance of the grout in (m·K)/W; T_m is the fluid mean temperature in K or °C; and T_b is the borehole wall average temperature in K or °C.

As R_b is estimated from the TRT results, the only unknown parameter of the equation (7) is the contact thermal resistance between the outer surface of the pipe and internal surface of the grout in contact with each pipe (a_{p-g}). The procedure and equations used to obtain its value are included in the equation (8) and the equations associated to it. The properties of the heat carrier water at 30 °C are estimated from existing bibliography [25]. For simple and double U pipe disposition, many authors proposed different estimation formulae to determine the effective internal thermal resistance of the grout, R_g as summarized by Raymond et al. [26] and Lamarche et al. [27]. In this case, equation (8.1) is used, which permits the estimation of the thermal resistance of the grout in contact with each pipe, according to the Thermal Resistance and Capacity Model proposed by Bauer et al. [28]. Equations (8.2) and (8.3) are extensively used to determine the thermal resistance of the pipe and the convection thermal resistance between the fluid and the pipe, respectively. Finally, equation (8.4) estimates the film coefficient according to the Dittus Boelter correlation [29].

$$a_{p-g} = 4 \cdot R_b - R_f - R_p - R_g \tag{8}$$

$$R_g = \frac{\cosh^{-1}\left[\frac{d_b^2 + d_{p,o}^2 - s^2}{2 \cdot d_b \cdot d_{p,o}}\right]}{(2 \cdot \pi \cdot \lambda_g)} \cdot \left[3.098 - 4.432 \cdot \frac{s}{d_b} + 2.364 \frac{s^2}{d_b^2}\right] \tag{8.1}$$

$$R_p = \frac{1}{2\pi\lambda_p} \ln\left(\frac{d_{p,o}}{d_{p,i}}\right) \tag{8.2}$$

$$R_f = \frac{1}{\pi d_{p,i} h_f} \tag{8.3}$$

$$h_f = \frac{4\lambda_w}{d_{p,i}} 0.023 \cdot Re^{0.8} \cdot Pr^{0.33} \tag{8.4}$$

Equation (6)

Finally, the uncertainty of the estimated λ_{ground} and R_b are calculated based on the method proposed by the European cooperation for accreditation [29]. The method is similar to that used by Sharqawy et al. [30] and Raymond et al. [31]. For the determination of the estimated uncertainties, the worst case scenario of the test carried out was chosen for the measured parameters.

3. RESULTS AND DISCUSSION

Four TRTs have been performed in 4 different borehole heat exchangers, each of them containing a different grouting material, to determine the thermal conductivity of the ground and the borehole thermal resistance.

3.1. Apparent thermal conductivity of the ground

The results of the four TRTs and the corresponding 5 to 48 h regression analyses are shown in Fig. 5. The effective thermal conductivity values obtained are 2.38 W/(m·K), 2.58 W/(m·K), 2.26 W/(m·K) and 2.20 W/(m·K). As all the tests are carried out for the same ground, all the thermal conductivities should have a similar value. All the TRTs except G2 present the same tendency and similar values for the effective thermal conductivity, with a maximum difference of 7.7%. G2 exhibits a slightly higher value than the rest of the tests, influenced by a heavy rainstorm that occurred right after the beginning of the test (a 9% deviation is calculated with respect to the mean value of all the tests), which probably wetted the higher layers underground, improving the thermal transmission and resulting in a higher measured final thermal conductivity. Mean value and standard deviation of the G1, G3 an G4 test sample are 2.28 W/(m·K) and 0.05 W/(m·K),respectively, so the probability of G2 being higher than the rest of the tests is of 91%.

The whole borehole field will be covered by concrete after carrying out these tests, resulting in an impervious layer that will prevent abrupt changes in the water content of the ground. Therefore, designing with the value of the second TRT might lead to an overestimation of the apparent thermal conductivity.

However, the higher value determined by G2 indicates the influence of the water table on the measured thermal conductivity. For instance, during the dry season, effective thermal conductivity of the ground might be lower than that registered during the wet season.

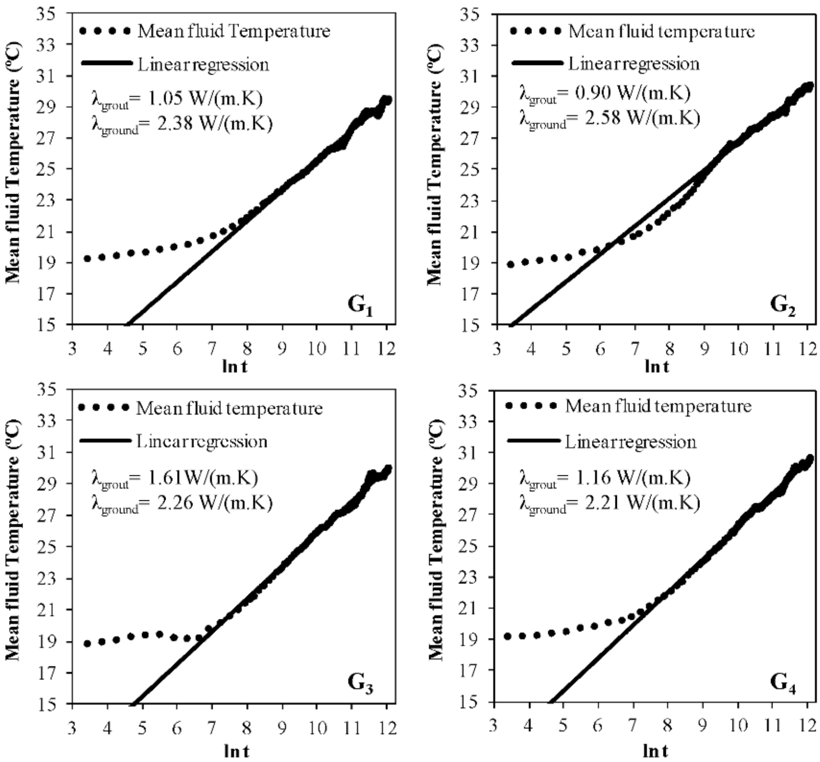

Fig. 5. Results obtained for each of the 4 TRTs done.

3.2. Borehole thermal resistance

Before the determination of the borehole thermal resistance, it is necessary to estimate the undisturbed ground temperature. Fig. 6 shows the vertical temperature profiles observed just before carrying out each TRT. All the profiles show similar values, which rules out any influence of any test on the following ones. For all the profiles a sharp decrease in the ground temperature is observed in the first 2 m of depth indicating a great influence of the ambient temperature over this interval. Therefore, this interval is not taken into consideration for the determination of T0. Mean undisturbed ground temperature values for G1, G2, G3 and G4 are 16.2 °C, 16.1 °C, 16.1 °C and 16.2 °C; higher than the mean ambient temperature registered the previous year, 13.9 C. As expected, the temperature of the first 20 m is affected by the ambient temperature conditions. Since all the TRTs were performed in July 2011, the minimum temperature is found to be at 25 m depth. From 30 m deep to the bottom of the borehole, linear temperature to depth gradient (DH/DT) is detected due to the Earth's internal Heat Flux, whose results are also shown in Fig. 6.

Temperature to depth gradients are calculated by regression analysis of the 30-90 m depth interval, showing similar values in all the cases, close to the mean worldwide value (33 m/°C) [32]. Estimated EHF values for R1, G2, G3, and G4 are 0.081 W/m2, 0.088 W/m2, 0.076 W/m2 and 0.077 W/m2, which are alike in all the TRTs except G2. Since G1 and G2 have the same geothermal gradient, the reason for the higher EHF of the latter must be the higher estimated ground thermal conductivity, already attributed to the rainstorm. Nevertheless, all the EHF values are approximately 10% lower than the value predicted by the Atlas of Geothermal Resources in Europe, 0.09 W/m2, which is issued by the European Commission [20].

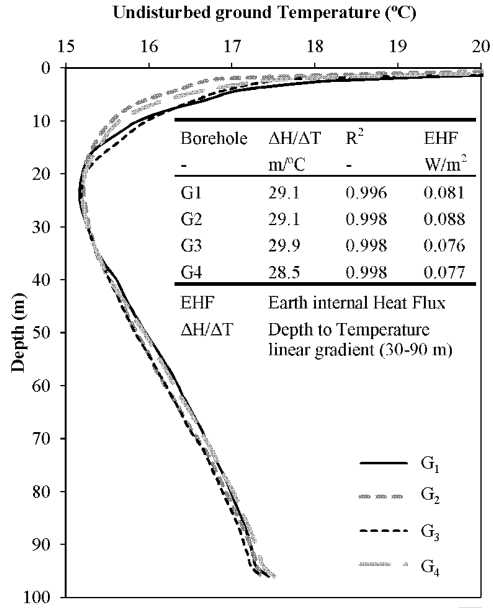

Fig. 6. Vertical temperature profiles for each TRT studied.

Fig. 7 illustrates the evolution in time of the estimated instantaneous R_b and the resulting 5 to 48 h mean value. The 90% confidence intervals of the estimated R_b values are shown in Fig. 8. The Borehole Thermal Resistances of the G1, G2 and G3 tests are significantly different among them, while the result in the G4 test is between the G1 and G4. According to the thermal conductivities measured in the grouts (λ_{grout}), the lowest thermal resistance was expected in G3. However, both G1 and G2 had lower values. Table 2 shows the results obtained for R_b, R_f, R_p, R_g and $a_{p\text{-}g}$.

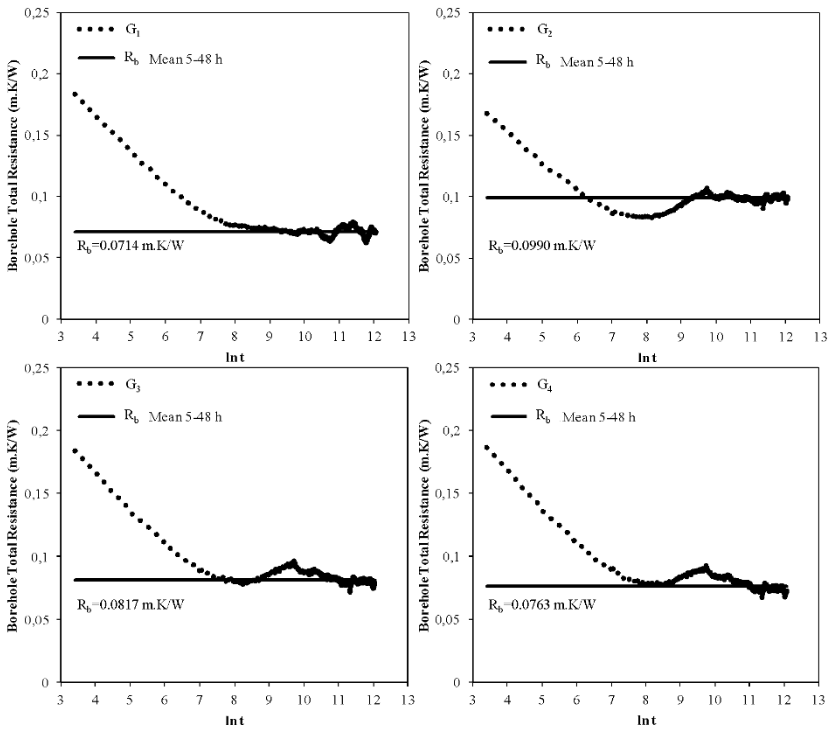

Fig. 7. Borehole total resistance (R_b) evolution during the tests.

As water flow rate and pipe type, disposition and shank spacing (s) are the same for all the cases evaluated, only thermal conductivity of the grout and $a_{p\text{-}g}$ could be responsible for the differences observed among the R_b values. As a consequence, for the same $a_{p\text{-}g}$ value, R_b values should show the same tendency observed for the R_g. However, G1 and G2 have lower R_b than the G3, whose grout has the highest thermal conductivity and, therefore, the lowest R_g, so this unusual behavior must be because of a_{p-g}. During the grout injection process, cement-based grouts underwent segregation due to the mixer type used. Consequently, a higher shrinkage was expected in cement-based grouts compared to the G1, which leads to a higher contact thermal resistance, represented by the a_{p-g} value.

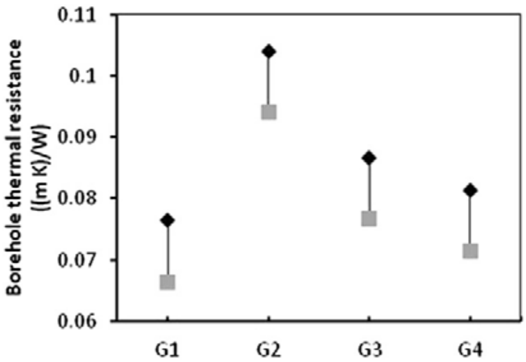

Fig. 8. 90% confidence interval of the borehole thermal resistances.

Table 2. Borehole thermal resistance broken down values for the TRTs evaluated.

Borehole	R_b	R_f	R_p	R_g	a_{p-g}
G_1	0.0714	0.0024	0.0796	0.1569	0.0467
G_2	0.0990	0.0024	0.0796	0.1830	0.1310
G_3	0.0817	0.0024	0.0796	0.1030	0.1418
G_4	0.0763	0.0024	0.0796	0.1420	0.0812

Finally the validity of the initial time chosen for the estimation of the ground thermal conductivity is analyzed, which is based on estimations. An insufficient initial time implies that the ground thermal conductivity may be influenced by the borehole configuration. To discard this possibility, R_b and resulting ground thermal conductivities are compared. If any relation exists an increase of the ground thermal conductivity should cause a decrease on the estimated R_b. G1 and G2 have the lowest and highest R_b, so the corresponding ground thermal conductivity values should also be the extremes of the TRTs performed. However, both G3 and G4 have intermediate R_b values but the ground's thermal conductivity is lower than that observed in G1. Therefore, and based on the TRTs studied, there is no evidence of any relation between R_b and the ground's thermal conductivity and the initial time seems adequate.

4. CONCLUSIONS

Cement-bentonite-graphite mix (G1) and 3 different cement based mortars containing Blast Oxygen Furnace slag (G2), silica sand (G3) and Construction and Demolition Waste (G4) as their main aggregates have been used to determine their influence on the thermal behavior of Geothermal Closed Loop Heat Exchangers. For that purpose, 4 TRTs were studied in 4 different Vertical Heat Exchangers to determine the influence of the grouting material on the thermal conductivity of the ground and the borehole thermal resistance. Based on the analysis of the data, the authors reached the following conclusions:

- Apparent thermal conductivity of the ground has been estimated for 3 different boreholes containing different grouting materials. The Thermal Response Test in the 3 different boreholes showed a mean thermal conductivity value of 2.28 W/(m·K) and a standard deviation of 0.05 W/(m·K).

- The second Thermal Response Test displays 9% increase in the thermal conductivity estimation, which was due to a rainstorm that occurred immediately after the beginning of the test. The rainstorm influenced the water content of the ground close to the surface, and water filtration could improve the thermal transmission of the ground.
- Vertical temperature profiles have been determined to calculate the ground's mean initial temperature and the undisturbed ground temperature gradient. Once thermal conductivity of the ground is estimated by the TRT, internal heat flux of the area is estimated, presenting a mean value of 0.08 W/m2.
- Thermal resistance results show that G1 mix performs better than the cement-based grouting materials. However, this phenomenon could be attributed to the segregation problems that affect the latter during the injection process. The higher thermal conductivity of the cement-based grouting materials does not compensate for the increase in the contact resistance between the pipes and the grout.

Acknowledgements

The authors wish to acknowledge the support provided by the GITECO Research Group of Construction Technology of the University of Cantabria and the Department of Construction at the University of Oviedo. Authors also want to acknowledge the technical support provided by Daniel Muñoz Sanz and Antonio Tébar (Sika S.A.U.) during the construction of the installation. The research project 'Development of systems for rainwater catchment and storage through the use of permeable pavements to assess its non-potable uses as a resource of low-enthalpy geothermal energy (REV)' [BIA2009-08272] of the University of Cantabria is possible thanks to the finance of the Research, Development and Innovation State Secretary of the Spanish Ministry for Economy and Competitiveness. Finally, authors wish to acknowledge the financial support provided by the research projects FICYT FC-10-EQUIP10-17 and BIA-2008-00058.

References

[1] A.M. Omer. Energy, environment and sustainable development, Renewable and Sustainable Energy Reviews, 12 (2008) 2265-2300.

[2] A. Mustafa Omer. Ground-source heat pumps systems and applications, Renewable and Sustainable Energy Reviews 12 (2008) 344-371.

[3] N. Nagai. S. Miyamoto, T. Tsuda, S. Yamahata, Experimental demonstrations and optimal design conditions of snow-melting system using geothermal and solar energy, Proceedings of the ASME Summer Heat Transfer Conference 2009, 3, 2009, pp. 767-771.

[4] A. Balbay, M. Esen, Experimental investigation of using ground source heat pump system for snow melting on pavements and bridge decks, Scientific Research and Essays 5 (24) (2010) 3955e3966.

[5] Y. Seo, U. Seo, J. Eum, S. Lee. Development of a geothermal snow melting system for highway overlays and its performance validations, Journal of Testing and Evaluation 39 (2011).

[6] W.A. Austin. Development of an in Situ System for Measuring Ground Thermal Properties, Oklahoma State University, Stillwater, Oklahoma, USA, 1998.

[7] S. Rainieri, F. Bozzoli, G. Pagliarini. Modeling approaches applied to the thermal response test: a critical review of the literature, HVAC and R Research 17 (6) (2011) 977-990.

[8] M.L. Allan, A.J. Philippacopoulos. Thermally Conductive Cementitious Grouts for Geothermal Heat Pumps. FY 1998 Progress Report, BNL 66103 (1998).

[9] M.L. Allan, S.P. Kavanaugh. Thermal conductivity of cementitious grouts and impact on heat exchanger length design for ground source heat pumps, HVAC and R Research 5 (1999) 87-98.

[10] M.L. Allan, A.J. Philippacopoulos. Properties and Performance of Cement-based Grouts for Geothermal Heat Pump Applications, Final Report, 1999.

[11] M.L. Allan. Materials characterization of superplasticized cement-sand grout, Cement and Concrete Research 30 (2000) 937-942.

[12] M.L. Allan, A.J. Philippacopoulos. Performance Characteristics and Modelling of Cementitious Grouts for Geothermal Heat Pumps (2000).

[13] C. Lee, K. Lee, H. Choi, H. Choi. Characteristics of thermally-enhanced bentonite grouts for geothermal heat exchanger in South Korea, Science China Technological Sciences 53 (2010) 123-128.

[14] F. Delaleux, X. Py, R. Olives, A. Dominguez. Enhancement of geothermal borehole heat exchangers performances by improvement of bentonite grouts conductivity, Applied Thermal Engineering 33-34 (2012) 92-99.

[15] M.D. Smith, R.L. Perry. Borehole grouting: field studies and thermal performance testing, ASHRAE Transactions 105 (1999) 451-457.

[16] Q. Zhang, W.E. Murphy. Measurement of thermal conductivity for three borehole fill materials used for GSHP, ASHRAE Transactions 106 (2000) 434-441.

[17] C. Lee, M. Park, S. Min, S.-. Kang, B. Sohn, H. Choi. Comparison of effective thermal conductivity in closed-loop vertical ground heat exchangers, Applied Thermal Engineering 31 (2011) 3669-3676.

[18] R. Borinaga-Treviño, P. Pascual-Muñoz, D. Castro-Fresno, J.J. Del Coz-Díaz. Study of different grouting materials used in vertical geothermal closed loop heat exchangers, Applied Thermal Engineering 50 (1) (2012) 159-167.

[19] ASTM D-5334-08, Standard Test Method for Determination of Thermal Conductivity of Soil and Soft Rock by Thermal Needle Procedure, American Society for Testing and Materials, 2008.

[20] S. Hurter, R. Haenel. Atlas of Geothermal Resources in Europe, Official Publications of the European Communities, Luxemburg, 2002.

[21] P. Mogensen. Fluid to duct wall heat transfer in duct heat storages. Proceedings of the International Conference on Subsurface Heat Storage in Theory and Practice, Swedish Council for Building Research, 1983, pp. 652-657.

[22] S.E.A. Gehlin, G. Hellström. Comparison of four models for thermal response test evaluation, ASHRAE Transactions 109 (1) (2003) 131-142.

[23] VDI 4620. Thermal Use of the Underground: Fundamentals, Approvals, Environmental Aspects, Verein Deutscher Ingenieure, 2000.

[24] C.P. Remund. Borehole thermal resistance: laboratory and field studies, ASHRAE Transactions 105 (1999) 439-445.

[25] J.P. Holman. Heat Transfer, Mc Graw Hill, Madrid, 1999.

[26] J. Raymond, R. Therrien, L. Gosselin. Borehole temperature evolution during thermal response tests, Geothermics 40 (2011) 69-78.

[27] L. Lamarche, S. Kajl, B. Beauchamp. A review of methods to evaluate borehole thermal resistances in geothermal heat-pump systems, Geothermics 39 (2010) 187-200.

[28] D. Bauer, W. Heidemann, H. Müller-Steinhagen, H.-.G. Diersch. Thermal resistance and capacity models for borehole heat exchangers, International Journal of Energy Research 35 (2011) 312-320.

[29] EA-4/02: Expression of the Uncertainty of Measurement in Calibration, European Co-operation for Acreditation, 1999.

[30] M.H. Sharqawy, E.M. Mokheimer, M.A. Habib, H.M. Badr, S.A. Said. Energy, exergy and uncertainty analyses of the thermal response test for a ground heat exchanger, International Journal of Energy Research 33 (2009) 582-592.

[31] J. Raymond, R. Therrien, L. Gosselin, R. Lefebvre. A review of thermal response test analysis using pumping test concepts, Ground Water 49 (2011) 932-945.

[32] G. Llopis Trillo, V. Rodrigo Angulo. Guía De La Energía Geotérmica, Comunidad de Madrid, Madrid, Spain, 2008.